

Probe Report

Title: Selective Small Molecule Inhibitors of 12-human lipoxygenase (12-hLO)

Authors: Ganesha Rai¹, Ajit Jadhav,¹ Lena Schultz,¹ Victor Kenyon,² William Leister,¹ Anton Simeonov,¹ Theodore R. Holman², David J. Maloney¹

¹ NIH Chemical Genomics Center, 9800 Medical Center Dr., Building B, Bethesda, MD, 20892-3370

² University of California, Santa Cruz

Version: #3

Date Submitted: 3/16/11

Assigned Assay Grant #: MH08128301

Screening Center Name & PI: NIH Chemical Genomics Center, Christopher P. Austin

Chemistry Center Name & PI: NIH Chemical Genomics Center, Christopher P. Austin

Assay Submitter & Institution: Dr. Theodore Holman, University of California at Santa Cruz

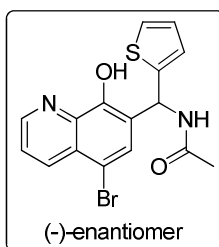
PubChem Summary Bioassay Identifier (AID): 2164

Abstract:

Human lipoxygenases (hLOs) are distributed among a variety of tissues and cellular locations in the body, and they are part of the first committed step in a cascade of metabolic pathways. As such, hLOs are implicated in the onset of inflammatory diseases such as cancers, heart disease and asthmas, making them an ideal target for pharmaceutical intervention. The lipoxygenase platelet-type 12-(*S*)-hLO has been implicated in skin diseases, diabetes, platelet hemostasis, thrombosis and cancer. Despite the potential of 12-hLO as a therapeutic target, potent and selective inhibitors of the enzyme are lacking in the patent or public literature. To date, the only known modulators of 12-hLO are either weak inhibitors or promiscuous polyphenolic compounds that inhibit several of the closely related isoymes. In this report, we describe the development of small-molecule inhibitors that exhibit nanomolar potency against 12-hLO and >50-fold selectivity over the related lipoxygenases and cyclooxygenases. Kinetic experiments indicate that this chemotype is a non-competitive inhibitor that does not reduce the active site iron. Moreover, chiral HPLC separation of several of the racemic lead molecules revealed a

strong preference for the (-)-enantiomer ($IC_{50} \sim 0.4\mu M$) compared to $> 25\mu M$ for the (+)-enantiomer, indicating a fine degree of selectivity in the active site due to chiral geometry. The small molecule probe ML127 (CID 44460175) and its related analogs represent the most potent and selective 12-hLO inhibitors reported thus far.

Probe Structure & Characteristics:



ML127

CID/ML#	Target Name	IC_{50}/EC_{50} (nM) [SID, AID]	Anti-target Name(s)	IC_{50}/EC_{50} (μM) [SID, AID]	Fold Selective	Secondary Assay(s) Name: IC_{50}/EC_{50} (nM) [SID, AID]
44460175/ ML127	12-hLO	430 nM [SID: 85736374, AID:1452]	15-hLO-1	30000 nM [SID: 85736374, AID:2157]	>70:1 (based on secondary assay)	12-hLO Cuvette Assay: 430 nM [SID: 85736374, AID:2155]
			15-hLO-2	250000 nM [SID:85736374, AID:881]	>581:1 (based on secondary assay)	[SID: 85736374]

Recommendations for scientific use of the probe:

ML127 is expected to be used by researchers studying inflammatory response mechanisms, human pancreatic beta-cell death during the progression of type 1 diabetes, and tumor angiogenesis. The characterized probe will be useful as a tool to study the biological role of 12-hLO in lipid- and prostaglandin-mediated signaling as related to inflammation, human platelet reactivity, progression of type 1 diabetes, and clot formation. One recent hypothesis on the inhibition of 12-hLO as a therapeutic target proposes that inhibition of 12-hLO slows down the progression of human beta-cell death in type 1 diabetes; another proposes that an inhibitor of 12hLO can be a blood-thinning agent devoid of dangerous

side effects, such as the promotion of excessive bleeding. ML127 provides a potent tool compound to validate such hypotheses.



1 Introduction

Lipoxygenases are a class of non-heme iron-containing enzymes. There are three major human lipoxygenases: 5-, 12-, and 15-hLO, whose primary enzymatic difference lies in their site-specific oxidation of arachidonic acidⁱ. The products of lipoxygenases are precursors of hormones such as leukotrienes and lipoxins, which have been implicated as critical in a variety of inflammatory diseases and cancers. Human lipoxygenases (hLOs) are distributed among a variety of tissues and cellular locations and have been implicated in numerous disease states. 5-hLO shuttles between the cytosol and nuclear membraneⁱⁱ and has been implicated in cancerⁱⁱⁱ and asthma^{iv}. Reticulocyte 15-hLO-1 has been implicated in colorectal^v and prostate^{vi} cancers, while epithelial 15-hLO-2 is expressed in hair, prostate, lung and cornea^{vii} and has demonstrated an inverse correlation of expression and prostate cancer^{viii}. Mutations in epidermis-type lipoxygenase-3 and 12-(*R*)-hLO, which are expressed in the skin, have been shown to cause non-bullous congenital ichthyosiform erythroderma^{ix}. Platelet-type 12-(*S*)-hLO (12-hLO), on which the current study focuses, has been implicated in skin disease,^x pancreatic,^{xi} breast^{xii} and prostate cancers.

Recently, 12-hLO has been implicated in the amplification of inflammatory response in type I diabetes, ultimately leading to the destruction of beta cells^{xiii}. Previous studies have demonstrated elevated 12-hLO mRNA expression levels in cancerous prostate tissue cell lines; also, addition of 12-hydroxyeicosatetraenoic acid (12-HETE) to human prostate adenocarcinoma cells increased their motility and their ability to invade neighboring tissues^{xiv}. These data have been supplemented with recent data demonstrating that 12-hLO enhances the excretion and expression of vascular endothelial growth factor (VEGF) under hypoxic conditions by up-regulating the protein level, mRNA and functionality of hypoxia inducible factor-1 alpha, a transcription factor that up-regulates VEGF activity^{xv}. Taken together, these studies suggest a very strong case for the involvement of 12-hLO in prostate cancer. Additional reports have implicated 12-hLO in breast cancer. 12-hLO mRNA was found to have increased expression in breast cancer tissue cell

lines^{xvi} versus noncancerous breast epithelial cell lines, where the addition of the LO inhibitor cinnamyl-3,4-dihydroxy- α -cyanocinnamate dramatically inhibited the growth of the breast cancer cell lines. Increased expression of 12-hLO mRNA has also been witnessed in tissues extracted from patients with breast cancer^{xvii}, versus healthy adjacent tissue.

2 Materials and Methods

General Chemistry: Unless otherwise stated, all reactions were carried out under an atmosphere of dry argon or nitrogen in dried glassware. Indicated reaction temperatures refer to those of the reaction bath, while room temperature (rt) is noted as 25°C. All solvents were of anhydrous quality, purchased from Aldrich Chemical Co., and used as received. Commercially available starting materials and reagents were purchased from Aldrich and were used as received. Analytical thin layer chromatography (TLC) was performed with Sigma Aldrich TLC plates (5x 20cm, 60 Å, 250 μ m). Visualization was accomplished by irradiation under a 254nm UV lamp. Chromatography on silica gel was performed using forced flow (liquid) of the indicated solvent system on Biotage KP-Sil pre-packed cartridges and using the Biotage SP-1 automated chromatography system. ¹H- and ¹³C NMR spectra were recorded on a Varian Inova 400 MHz spectrometer. Chemical shifts are reported in ppm with the solvent resonance as the internal standard (CDCl₃ 7.26 ppm, 77.00 ppm, DMSO-*d*₆ 2.49 ppm, 39.51 ppm for ¹H, ¹³C respectively). Data are reported as follows: chemical shift, multiplicity (s = singlet, d = doublet, t = triplet, q = quartet, brs = broad singlet, m = multiplet), coupling constants, and number of protons. Low resolution mass spectra (electrospray ionization) were acquired on an Agilent Technologies 6130 quadrupole spectrometer coupled to the HPLC system. High resolution mass spectral data were collected in-house using an Agilent 6210 time-of-flight mass spectrometer, also coupled to an Agilent Technologies 1200 series HPLC system. If needed, products were purified via a Waters semi-preparative HPLC equipped with a Phenomenex Luna[®] C18 reverse phase (5 micron, 30x 75mm) column having a flow rate of 45 ml/min. The mobile phase was a mixture of acetonitrile (0.025% TFA) and H₂O (0.05% TFA), and the temperature was maintained at 50°C.

Samples were analyzed for purity on an Agilent 1200 series LC/MS equipped with a Luna® C18 reverse phase (3 micron, 3x 75mm) column having a flow rate of 0.8-1.0 ml/min over a 7-minute gradient and a 8.5 minute run time. Purity of final compounds was determined to be >95%, using a 3µl injection with quantitation by AUC at 220 and 254nm (Agilent Diode Array Detector).

Biological Reagents: All commercial fatty acids (Sigma-Aldrich Chemical Company) were re-purified using a Higgins HAIsil Semi-Preparative (5µm, 250 × 10mm) C-18 column. Solution A was 99.9% MeOH and 0.1% acetic acid; solution B was 99.9% H₂O and 0.1% acetic acid. An isocratic elution of 85% A:15% B was used to purify all fatty acids, which were stored at –80°C for a maximum of 6 months.

Over expression and Purification of 12-Human Lipoxygenase, 5-Human Lipoxygenase, 12/15-Mouse Lipoxygenase and the 15-Human Lipoxygenases: Human platelet 12-lipoxygenase (12-hLO), human reticulocyte 15-lipoxygenase-1 (15-hLO-1), and human epithelial 15-lipoxygenase-2 (15-hLO-2), were expressed as N-terminally, His₆-tagged proteins and purified to greater than 90% purity, as evaluated by SDS-PAGE analysis. Human 5-lipoxygenase was expressed as a non-tagged protein and used as a crude ammonium sulfate protein fraction, as published previously. 12/15-mouse lipoxygenase (12/15-mLO) was expressed as a non-tagged protein and purified on Bio-Rad Uno Q1 with NaCl as the eluent. Iron content of 12-hLO (7 µM) was determined with a Finnigan inductively coupled plasma mass spectrometer (ICP-MS), using cobalt-EDTA as an internal standard. Iron concentrations were compared to standardized iron solutions and used to normalize enzyme concentrations.

High-throughput Screen Materials: Dimethyl sulfoxide (DMSO) ACS grade was from Fisher, while ferrous ammonium sulfate, Xylenol Orange (XO), sulfuric acid, and Triton X-100 were obtained from Sigma-Aldrich.

2.1 Assays

Quantitative High Throughput Screen for Inhibitors of 12-hLO: All screening operations were performed on a fully integrated robotic system (Kalypsys Inc, San Diego, CA) as described elsewhere^{xviii}. Three µl of enzyme (approximately 80nM 12-hLO, final concentration) was

dispensed into 1536-well Greiner black clear-bottom assay plates. Compounds and controls (23 nl) were transferred via Kalypsys PinTool equipped with 1536-pin array (See Table 1 for protocol details). The plate was incubated for 15 min at room temperature, and then a 1 μ l aliquot of substrate solution (50 μ M arachidonic acid final concentration) was added to start the reaction. The reaction was stopped after 6.5 min by the addition of 4 μ l FeXO solution (final concentrations of 200 μ M Xylenol Orange (XO) and 300 μ M ferrous ammonium sulfate in 50mM sulfuric acid). After a short spin (1000 rpm, 15 sec), the assay plate was incubated at room temperature for 30 minutes. The absorbances at 405 and 573 nm were recorded using ViewLux high throughput CCD imager (Perkin-Elmer, Waltham, MA) using standard absorbance protocol settings. During dispense, enzyme and substrate bottles were kept submerged into a +4 $^{\circ}$ C recirculating chiller bath to minimize degradation. Plates containing DMSO only (instead of compound solutions) were included approximately every 50 plates throughout the screen to monitor any systematic trend in the assay signal associated with reagent dispenser variation or decrease in enzyme specific activity.

Data was analyzed in a similar method as described elsewhere. Briefly, assay plate-based raw data was normalized to controls, and plate-based data corrections were applied to filter out background noise. All concentration response curves (CRCs) were fitted using in-house developed software (<http://ncgc.nih.gov/pub/openhts/>). Curves were categorized into four classes: complete response curves (Class 1), partial curves (Class 2), single point actives (Class 3) and inactives (Class 4). Compounds with the highest quality, Class 1 and Class 2 curves, were prioritized for follow-up. PubChem AID: 1452.

Table 1: 12-hLO qHTS assay protocol for 1536-well plate format

Step	Parameter	Value	Description
1	Reagent	3 μ L	Enzyme: 120 nM 12-hLO final conc.
2	Compound	23 nL	Compound library
3	Control	23 nL	Intraplate titration
4	Incubation time	15 min	Compound interaction with target
5	Reagent	1 μ L	Substrate: AA 40 μ M final conc.
6	Incubation time	5 min	Enzymatic reaction
7	Reagent	4 μ L	Stop solution
8	Time, speed	15 sec, 1000 rpm	Centrifugation
9	Incubation time	30 minutes	Chromogenic detection development
10	Assay readout	405 and 573 nm	ViewLux absorbance read

Step	Notes
1	Black clear-bottom plates, single tip dispense, enzyme in columns 1, 2, 5-48, vehicle in column 3 and 4.
2	Pintool transfer of compounds to assay plate columns 5-48. 57.5 μ M to 0.7 nM titration series.
3	Pintool transfer of control inhibitor to column 2. Three-fold, 16 pt dilution in duplicate.
4	Room temperature incubation in auxiliary hotel.
5	4-tip dispense of arachidonic acid (AA), 1536 wells.
6	Room temperature incubation in auxiliary hotel.
7	4-tip dispense of divalent iron/xylenol orange in dilute sulfuric acid, 1536 wells.
8	Plate centrifugation to remove bubbles.
9	Room temperature incubation in auxiliary hotel.
10	Endpoint measurement of reaction progress.

Lipoxygenase UV-Vis Assay: The initial one-point inhibition percentages were determined by following the formation of the conjugated diene product at 234nm ($\epsilon = 25,000 \text{ M}^{-1}\text{cm}^{-1}$) with a Perkin-Elmer Lambda 40 UV/Vis spectrophotometer at one inhibitor concentration. All reactions were 2ml in volume and constantly stirred using a magnetic stir bar at room temperature (23°C) with approximately 40nM for 12-hLO (by iron content), 20nM of 15-hLO-1 (by iron content), 1 μ M for 15-hLO-2 (by Bradford). Reactions with 12-hLO were carried out in 25mM HEPES (pH 8.0) 0.01% Triton X-100 and 10 μ M AA. Reactions with the crude, ammonium sulfate precipitated 5-hLO were carried out in 25mM HEPES (pH 7.3), 0.3mM CaCl₂, 0.1mM EDTA, 0.2mM ATP, 0.01% Triton X-100 and 10 μ M AA. Reactions with 15-hLO-1 and 15-hLO-2 were carried out in 25mM HEPES buffer (pH 7.5), 0.01% Triton X-100 and 10 μ M AA. The concentration of AA (for 5-hLO, 12-hLO and 15-hLO-2) was quantitatively determined by allowing the enzymatic reaction to go to completion. IC₅₀ values were obtained by determining the enzymatic rate at various inhibitor concentrations and plotted against inhibitor concentration, followed by a hyperbolic saturation curve fit. PubChem AID: 2163.

Fluorescence Iron Binding Assay: Fluorescence readings were taken with a Perkin Elmer Luminescence Spectrometer LS 50 B in the presence and absence of iron with the excitation maximum $\epsilon_{\text{ex}} = 360\text{nm}$ and the emission maximum $\epsilon_{\text{em}} = 410\text{nm}$. The excitation slit was set at 5nm and the emission slit was set at 10nm. Due to the low intensity of the fluorophore, the filter was kept open. As a control, 1mM 8-HQ-5-sulfonic acid was dissolved in 25mM HEPES buffer (pH 8.5) and aliquoted to a 2ml cuvette. In a separate cuvette, 1mM 8-HQ-5-sulfonic acid and either 10 μ M Fe²⁺ (as [NH₄]₂[Fe][SO₄]₂·6H₂O) or Fe³⁺ (as Fe₂(SO₄)₃) in 25mM HEPES buffer (pH 8.5) was added and allowed to equilibrate for 5 minutes. For the experiment, 2ml of 1mM **1** was dissolved in 2mM HEPES buffer (pH 8.5) and the fluorescence intensity was taken. In a separate cuvette, 1mM **1** was dissolved in 25mM HEPES buffer (pH 8.5), incubated with less than 1 μ M (by iron content) of 12-hLO, and allowed to equilibrate for 5 minutes.

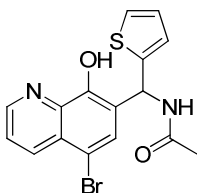
DPPH Antioxidant Test: Compounds were dissolved in dimethyl sulfoxide (DMSO) at 1-20mM concentration (1,000-fold concentrated). The antioxidant activity of these compounds was assayed by monitoring the quenching of the standard free radical 1.1-diphenyl-2-picrylhydrazyl (DPPH) upon reaction with the testing compounds. A known free radical scavenger, nordihydroguaiaretic acid (NDGA), was used as a positive control. To achieve a final

concentration of 5 μ M, ten microliters of 1mM testing reagents were added to 2ml of 500 μ M DPPH, stirring in a cuvette. Optical absorbance was monitored and recorded at 25-sec intervals as described elsewhere. The decrease in optical absorbance at 517nm was monitored using a Perkin-Elmer Lambda 40 spectrometer. The rate of reaction is proportional to the antioxidant potency of the test compounds.

Steady-State Inhibition Kinetics: Lipoygenase rates were determined by monitoring the formation of the conjugated product, 12-HPETE, at 234nm ($\epsilon = 25\,000\text{ M}^{-1}\text{ cm}^{-1}$) with a Perkin-Elmer Lambda 40 UV/Vis spectrophotometer. Reactions were initiated by adding approximately 80 nM 12-hLO to a constantly stirring 2ml cuvette containing 3 – 40 μ M AA in 25mM HEPES buffer (pH 7.5), in the presence of 0.01% Triton-X-100. The substrate concentration was quantitated by allowing the enzymatic reaction to proceed to completion. Kinetic data were obtained by recording initial enzymatic rates, at varied inhibitor concentrations, and subsequently fitted to the Henri-Michaelis-Menten equation, using KaleidaGraph (Synergy) to determine the microscopic rate constants, V_{\max} ($\mu\text{mol}/\text{min}/\text{mg}$) and V_{\max}/K_M ($\mu\text{mol}/\text{min}/\text{mg}/\mu\text{M}$). These rate constants were subsequently re-plotted and normalized to the iron content (120nM) as $1/k_{\text{cat}}$ and K_M/k_{cat} versus inhibitor concentration, to yield K_{iu} and K_{ic} , respectively.

Cyclooxygenase Assay: Ovine COX-1 (Cat. No. 60100) and human COX-2 (Cat. No. 60122) were purchased from Cayman chemical. Approximately 2 μ g of either COX-1 or COX-2 were added to buffer containing 100 μ M AA, 0.1M Tris-HCl buffer (pH 8.0), 5mM EDTA, 2mM phenol and 1 μ M hematin at 37°C. Data was collected using a Hansatech DW1 oxygen electrode chamber. Inhibitors were incubated with the respective COX for 20 minutes and added to the reaction mixture, and the consumption of oxygen was recorded. Ibuprofen and the carrier solvent, DMSO, were used as positive and negative controls, respectively.

2.2 Probe Chemical Characterization



Probe Characterization (CID44460175/ML127):

Purity >95% as judged by LC/MS and ¹H NMR

¹H NMR (DMSO-*d*₆) δ 1.94 (s, 3 H), 6.78 (dt, *J* = 3.5, 1.2 Hz, 1 H), 6.89 (dd, *J* = 8.9 and 1.1 Hz, 1 H), 6.93 (dd, *J* = 5.1 and 3.3 Hz, 1 H), 7.40 (dd, *J* = 5.1 and 1.4 Hz, 1 H), 7.74 (dd, *J* = 8.6, 4.1 Hz, 1 H), 7.95 (s, 1 H), 8.43 (dd, *J* = 8.5, 1.5 Hz, 1 H), 8.95 (dd, *J* = 4.1 and 1.6 Hz, 1 H), 9.00 (d, *J* = 8.8 Hz, 1 H), 10.46 (s, 1 H); ¹³C NMR (DMSO-*d*₆) δ 22.55, 45.35, 108.50, 123.41, 124.84, 125.08, 125.68, 126.34, 126.78, 129.38, 134.97, 138.89, 145.91, 149.24, 149.71 and 168.39; HRMS (*m/z*): [M + H]⁺ calcd. for C₁₆H₁₄BrN₂O₂S, 376.9954; found, 376.9956. (–)-*N*-((5-bromo-8-hydroxyquinolin-7-yl)(thiophen-2-yl)methyl)acetamide: [α]_D²³ = - 65.55 (c = 0.33, MeOH)

LC/MS conditions:

LC/MS (Agilent system) Retention time *t*₁ (short) = 3.42 min and *t*₂ (long) = 5.36.

Column: 3 x 75 mm Luna C18, 3 micron

Run time: 4.5 min (short); 8.5 min (long)

Gradient: 4% to 100%

Mobile phase: Acetonitrile (0.025% TFA), water (0.05% TFA).

Flow rate: 0.8 to 1.0ml

Temperature: 50°C

UV wavelength: 220nm, 254nm

MLS Numbers for probe analogs:

MLS IDs	NCGC IDs	SID	CID	ML
MLS002729016	NCGC00183685-01	99495752	44460175	*Probe compound ML127
MLS003370621	NCGC00188369-03	104224280	44460175	

MLS002729017	NCGC00183696-01	99495753	44142351
MLS002729018	NCGC00183691-01	99495754	2921053
MLS002729019	NCGC00183688-01	99495755	44460172
MLS002729020	NCGC00183690-01	99495756	44142346
MLS002729021	NCGC00183695-01	99495757	44460176

Table 2. Probe *in vitro* ADME properties:^a

Compound	aq. Kinetic sol. (PBS @ pH 7.4)	Caco-2 (P_{app} 10^{-6} m/s @ pH 7.4)	Efflux ratio (B→A)/(A→B)	Mouse liver microsome stability ($T_{1/2}$)	PBS-pH 7.4 stability: % remaining after 48h	Mouse plasma stability: % remaining after 48h
34	14.5 μ M	8.8	2.3	<10 min.	100	98.3

^akinetic solubility measurements were conducted at Analiza Inc. using nitrogen detection methodologies. Caco2 permeability, microsomal stability and mouse plasma stability experiments were conducted at Pharmaron Inc.

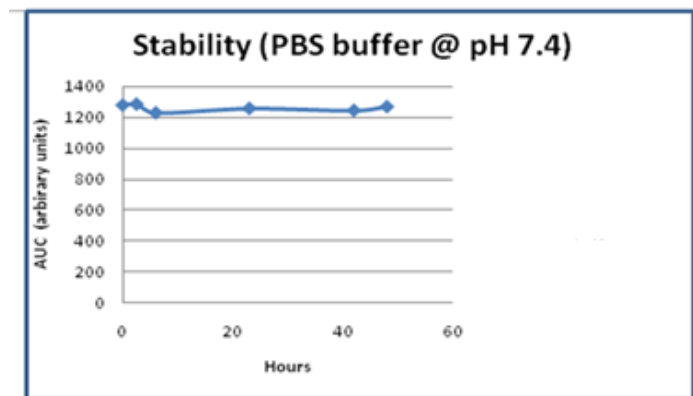
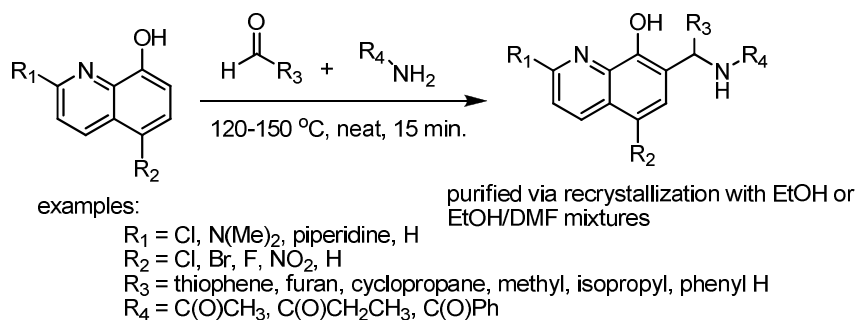


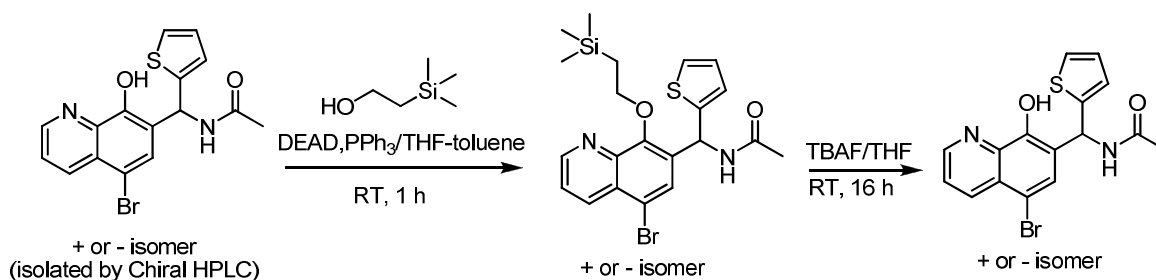
Figure 1. Buffer Stability (48 h @ 25°C) of (NCGC00183685-01/CID44460175/ML127), Percent remaining after 48h = 100%. AUC = area under the curve

2.3 Probe Preparation

Scheme 1: General synthetic route for access to racemic material



Scheme 2: Synthetic route required for the preparation of the chiral probe compound



General Procedure for the preparation of 8-HQ analogs: Differentially substituted-quinolin-8-ol (0.5g, 2.78mmol), amide, amine or aniline (2.92mmol) and the aldehyde (3.06mmol) were stirred neat at 120-150°C for 15 minutes. Upon heating, the reaction mixture melted, and solid was formed after completion of the reaction. The solid product was washed with ethyl acetate, and the crude product was purified by recrystallization from ethanol-DMF mixture.

Note: unprotected 8-HQ derivatives do not purify well on Chiral HPLC, so the phenolic hydroxyl group is protected as the trimethylsilyl ethyl ether.

Preparation of N-((5-bromo-8-(2-(trimethylsilyl)ethoxy)quinolin-7-yl)(thiophen-2-yl)methyl)acetamide: A mixture of N-((5-bromo-8-hydroxyquinolin-7-yl)(thiophen-2-yl)methyl)acetamide (3.09g, 8.2mmol, 1equiv), 2-(trimethylsilyl)ethanol (1.3ml, 9.0mmol, 1.1equiv), and triphenylphosphine (3.22g, 12.3mmol, 1.5equiv) in THF (30ml) and Toluene (10ml) was added 40% solution of DEAD in toluene (5.60ml, 12.3mmol, 1.5equiv) at room temperature. The reaction mixture was stirred at room temperature for 1 h. After completion of the reaction, excess solvent was removed under diminished pressure, and the crude product was purified on a biotage flash system. Elution with 20 % ethyl acetate in hexanes gave the pure product as a mixture of two isomers. The enantiomers were then separated on a chiral HPLC system using the method described below to get the (+) isomer (2nd peak) and (-) isomer (1st peak).

Separation of enantiomers via Chiral HPLC:

Analytical analysis: Analytical analysis was performed on a Chiralcel IA column (4.6 x 150mm, 5 micron). The mobile phase was 30% isopropanol in hexanes at 1.0 ml/min. The sample was detected with a diode array detector (DAD) at 220nm and 254nm. Optical rotation was determined with an in-line polarimeter (PDR-Chiral).

First eluting peak: 3.66 minutes; negative rotation

Second eluting peak: 4.31 minutes; positive rotation

Preparative Purification

Preparative purification was performed on a Chiralcel IA column (5x 50cm, 20 micron). The mobile phase was 30% isopropanol in hexanes at 35 ml/min. Fraction collection was triggered by UV absorbance (254nm).

Preparation of N-((5-bromo-8-hydroxyquinolin-7-yl)(thiophen-2-yl)methyl)acetamide (-)-enantiomer [Probe molecule]: A solution of the – isomer of N-((5-bromo-8-(2-(trimethylsilyl)ethoxy)quinolin-7-yl)(thiophen-2-yl)methyl)acetamide (0.83g, 1.74mmol, 1equiv) in THF (8ml) was added to a 1 M solution of TBAF in THF (3.8ml, 3.8mmol, 2.2equiv) and stirred at room temperature for 16 h. Excess solvent was evaporated, and the crude residue was

agitated with ice water. The precipitate was collected by filtration and washed thoroughly with water, then with cold ethanol. The solid material was allowed to dry under vacuum for 24 h, which yielded a white solid.

3 Results

3.1 Summary of Screening Results

The 12-hLO qHTS screen utilized 956 assay plates run interleaved in an uninterrupted robotic screening sequence. The signal-to-background ratio was on average 4.29, and the average Z' screening factor associated with each plate was 0.69, indicating a robust performance of the screen. The known lipoxygenase inhibitor nordihydroguaiaretic acid (NDGA) was included as an intraplate control on each assay plate to ascertain screening quality. The control inhibitor was added as a 16-point dilution series in duplicate between 115 μM and 8 pM, and control gave reproducible potency throughout the entire run, thus indicating a stable run. During this screen, 151,834 compounds were tested in at least 7 concentrations, ranging from 57.5 μM to 0.7 nM. For each well, the absorbance at 405 nm as well as at 573 nm was collected, resulting in 2.6 million data points. The 573-to-405 absorbance ratio was computed to follow enzyme activity and the corresponding effect of library compounds.

Following the qHTS, the concentration response curves (CRCs) data were subjected to a classification scheme to rank the quality of the CRCs as described by Inglese and co-workers. Briefly, the CRCs were placed in four classes. Class 1 contained complete concentration-response curves showing both upper and lower asymptotes and r^2 values greater than 0.9. Class 2 contained incomplete CRCs lacking the lower asymptote and showed $r^2 > 0.9$. Class 3 curves are of the lowest confidence, as they are defined by a single concentration point, where the minimal acceptance activity is set 3 SD of the mean activity calculated as described above. Finally, class 4 contained compounds that do not show any CRSs, and are therefore classified as inactives. Of the 151,834 screened compounds, 149,407 were regarded as inactives and 2,295 as inconclusive (Figure 2). 181 compounds were

classified as actives, belonging to curve classes -1.1, -1.2, -2.1 or -2.2. A subsequent cheminformatics analysis of the top inhibitors from the qHTS led to 67 clusters and 124

singletons that were active against 12-hLO. Compounds that were selective for 12-hLO were pursued for further optimization.

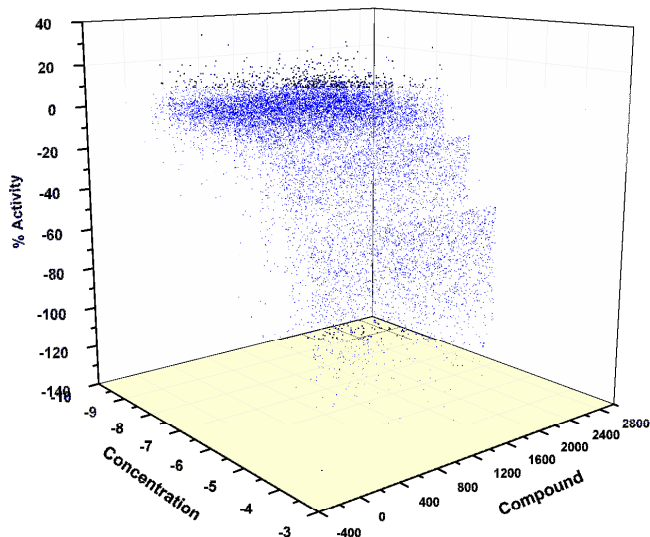
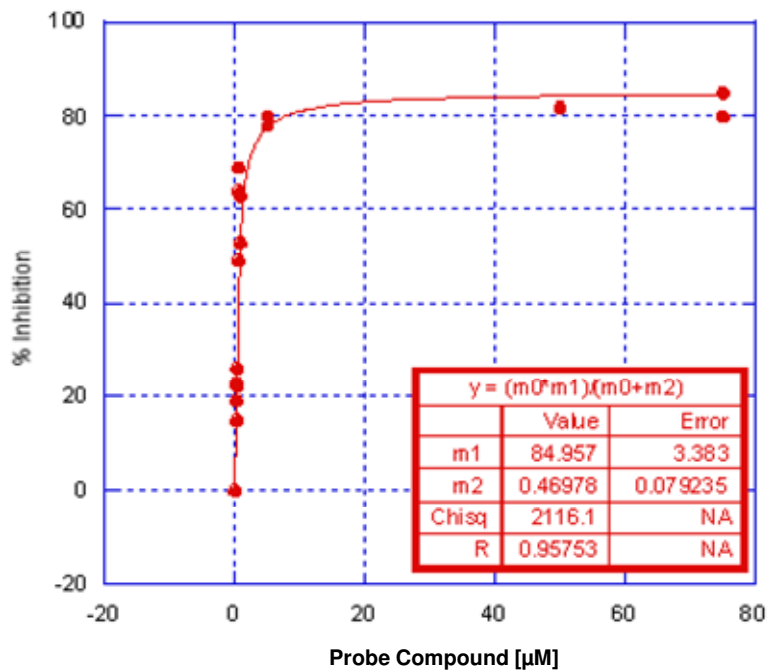


Figure 2: 3D scatter plot of inhibitors from 12-hLO qHTS. Concentration-response relationships for all active and inconclusive inhibitors are shown (1.6% of all compounds screened). Remaining 98.4% of compounds were inactive (not shown).

3.2 Dose Response Curves for Probe



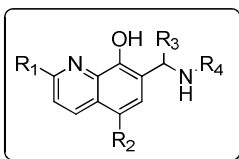
UV-Vis Assay Dose Response for ML127

3.3 Scaffold/Moiety Chemical Liabilities

Mechanistically, this chemotype has the potential of under-going a retro Mannich reaction to form a reactive intermediate (*vide infra*). However, we have shown that this compound is stable in both assay buffer and mouse plasma, so this does not appear to be an issue for this particular class of 7-substituted,8-HQs (see below for details).

3.4 SAR Tables

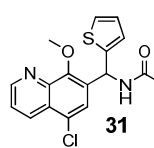
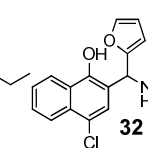
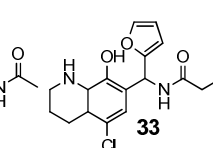
Table 3. SAR table for 12-hLO inhibition-Representative Analogs



Entry	CID	SID	NCGC IDs	R ₁	R ₂	R ₃	R ₄	Potency (μM) [± SD (μM)], n= replicates
1	2921716	85736364	NCGC00182956-01	H	NO ₂	thiophene	C(O)CH ₂ CH ₃	0.8 [0.2], n = 2
2	3136134	85736357	NCGC00182957-01	H	Cl	thiophene	C(O)CH ₂ CH ₃	1.0 [0.3], n = 2
3	2920793	85736379	NCGC00183692-01	H	Cl	thiophene	C(O)CH ₃	1.0 [0.1], n = 2
4	44460173	85736372	NCGC00183689-01	H	Br	thiophene	C(O)CH ₂ CH ₃	14 [4.0], n = 2
5	44460175	85736374	NCGC00183685-01	H	Br	thiophene	C(O)CH ₃	1.0 [0.2], n = 3
6	3136123	85736366	NCGC00182903-01	H	H	thiophene	C(O)CH ₂ CH ₃	3.4 [0.6], n = 2
7	44142351	85736386	NCGC00183696-01	H	F	thiophene	C(O)CH ₃	2 [0.2], n = 2
8	2921923	85736363	NCGC00182907-01	H	NO ₂	furan	C(O)CH ₂ CH ₃	1.2 [0.4], n = 2
9	2920571	50124408	NCGC00179686-01	H	Cl	furan	C(O)CH ₂ CH ₃	1.0 [0.2], n = 4
10	2921053	85736378	NCGC00183691-01	H	Cl	furan	C(O)CH ₃	3.0 [0.5], n = 3
11	44460172	85736371	NCGC00183688-01	H	Br	furan	C(O)CH ₂ CH ₃	1.9 [0.4], n = 2
12	44460174	85736373	NCGC00183684-01	H	Br	furan	C(O)CH ₃	2.0 [0.4], n = 3
13	44142359	85736385	NCGC00183702-01	H	F	furan	C(O)CH ₃	5.0 [1], n = 2
14	44142343	85736369	NCGC00183707-01	H	Cl	cyclopropane	C(O)CH ₂ CH ₃	1.6 [0.3], n = 2
15	44142346	85736377	NCGC00183690-01	H	Cl	cyclopropane	C(O)CH ₃	3.0 [0.6], n = 2
16	44142342	85736368	NCGC00183706-01	H	Cl	isopropyl	C(O)CH ₂ CH ₃	1.3 [0.4, n = 2]
17	44142345	85736376	NCGC00183687-01	H	Cl	isopropyl	C(O)CH ₃	2.6 [0.4], n = 2
18	44142341	85736367	NCGC00183704-01	H	Cl	methyl	C(O)CH ₂ CH ₃	~50, n = 2
19	44142344	85736375	NCGC00183686-01	H	Cl	methyl	C(O)CH ₃	>150, n = 1
20	44142348	85736382	NCGC00183716-01	H	F	methyl	C(O)CH ₃	>150, n = 1
21	44460178	85736388	NCGC00183712-01	H	Cl	H	C(O)CH ₃	>150, n = 1
22	44460168	85736359	NCGC00182958-01	H	Cl	5-Me-thiophene	C(O)CH ₂ CH ₃	3.5 [1], n = 2
23	44460167	85736358	NCGC00182906-01	H	Cl	5-bromofuran	C(O)CH ₂ CH ₃	>75, n = 1
24	2921053	85736378	NCGC00183691-01	Cl	Cl	furan	C(O)CH ₃	>150, n = 1
25	44460179	85736389	NCGC00183714-01	N(Me) ₂	Cl	furan	C(O)CH ₃	>150, n = 1
26	44460180	85736390	NCGC00183709-01	piperidine	Cl	furan	C(O)CH ₃	>150, n = 1
27	3136132	85736355	NCGC00182961-01	H	Cl	4-Me-Ph	C(O)CH ₂ CH ₃	>150, n = 1
28	44460169	85736360	NCGC00182905-01	H	Cl	4-F-Ph	C(O)CH ₂ CH ₃	>50, n = 1
29	46926342	99431504	NCGC00188371-01	H	Cl	furan	C(O)Ph	>25, n = 1
30	46926343	99431505	NCGC00188372-01	H	Cl	furan	C(O)-4-Me-Ph	>25, n = 1

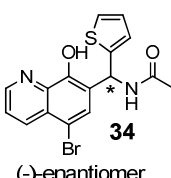
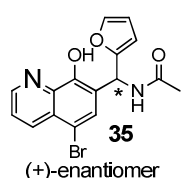
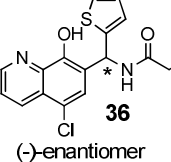
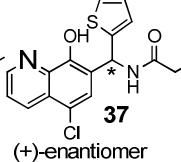
Note: All compounds in table were synthesized at NCGC.

Table 4. SAR table for 12-hLO inhibition-Representative Analogs

Entry	CID	SID	NCGC IDs	Potency (μM) [± SD (μM)], n= replicates
 31	44142340	85736380	NCGC00183694-01	>75, n = 1
 32	44142388	99431500	NCGC00183710-01	>75, n = 1
 33	46926341	99431501	NCGC00183728-01	3.0 [0.7], n = 2

Note: All compounds in table were synthesized at NCGC.

Table 5. SAR table for 12-hLO inhibition-Enantiomers

Entry	CID	SID	NCGC IDs	Potency (μM) [\pm SD (μM), n= replicates]	
	34	44460175	99431502	NCGC00188369-01	0.43 [0.04], n = 2
	35	44460175	99431503	NCGC00188370-01	>25, n = 2
	36	3136134	99431507	NCGC00188868-01	0.38 [0.05], n = 2
	37	3136134	99431506	NCGC00188867-01	>25, n = 2

Note: All compounds in table were synthesized at NCGC.

3.5 Cellular Activity

The probe molecule ML127 (NCGC00183685-01/CID44460175) is clearly cell permeable, with a $P_{\text{app}} \times 10^6/\text{cm}\cdot\text{s}^{-1}$ of 8.8 in Caco-2 cell lines, and does not appear to be susceptible to efflux, as the efflux ratio is ~ 2 .

3.6 Profiling Assays

The probe compound is inactive against LO isozymes (5-LO, 15-hLO-1 and 15-hLO-2) and closely related COX-1 and COX-2. Additionally, our probe compound has been tested in 18 other assays at NCGC and has been inactive in all of them.

4 Discussion

To investigate requirements for inhibition and potency, we prepared derivatives of the 8-HQ scaffold that were chemically modified at the R₁, R₂, R₃ and R₄ positions (see Table 3). In general, the scaffold of **1** was tolerant to a variety of changes in size and electrostatics in the R₂, R₃ and R₄ positions without dramatic changes in potency; however, there were several combinations of modifications that were not well tolerated.

Investigations of various substituents at R₃ revealed that compared to the thiophene or furan moiety, both smaller groups (R₃ = H, entry **21** and R₃ = Me, entries **18-20**) and larger groups (R₃ = 4-Me-Ph, entry **27** and R₃ = 4-F-Ph, entry **28**) resulted in essentially complete loss of activity. Thiophene, furan, cyclopropyl, cyclopentyl, and isopropyl groups all showed comparable activity.

Limited investigation at R₁ was conducted, but all modifications at this position led to loss in activity (entries **24-26**), suggesting that the binding pocket does not tolerate increased steric bulk in this position. Similarly, increasing the size of the substituents off the amine (R₄) was not favorable for improved potency, as shown with analogs **29** and **30** (R = C(O)Ph and C(O)-4-Me-Ph respectively). Additionally, [R₄ = C(O)CH(CH₃)₂ and C(O)(CH₂)₂CH₃] were synthesized, and these analogs also displayed weak potency (data not shown). In contrast, modification to R₂ was well tolerated with H, Cl, Br, F, NO₂, all of which showed comparable activity.

8-HQ scaffolds are known metal chelators,^{xix} and chelation of the LO active site iron has been documented in the literature previously^{xx}. Therefore, we probed the chemical requirements for metal chelation by modifying the oxygen and nitrogen ligands that could bind the active site iron (see entries **31-33**). Both methylation of the phenol (entry **31**) and removal of the ring nitrogen (entry **32**) resulted in a loss of potency. However, when the pyridine was replaced by a piperidine (**33**), a non-rigid heterocycle, the inhibition was not affected (IC₅₀ = 3.0 +/- 0.7 μM). These data are consistent with the inhibitors ligating the metal in a bidentate fashion, given that piperidines are comparable in ligand strength to pyridines, and that neither of the monodentate modifications of the 8-HQ core inhibit 12-hLO.

Our final investigation into the SAR around the 8-HQ scaffold was conducted to identify if the two enantiomers had differential potency. As such, we utilized normal-phase chiral HPLC to effectively separate the enantiomers of both analogs **2** and **5**. Interestingly, both (-)-**2** (aka **36-**) and (-)-**8** (aka **34**) displayed 12-hLO inhibition at approximately half the IC₅₀ value of the racemic mixture (**34** (probe molecule) (-)-enantiomer, IC₅₀ = 0.43 +/- 0.04 μM; (racemic) IC₅₀ = 1.1 +/- 0.1 μM; **36** (-)-enantiomer, IC₅₀ = 0.38 +/- 0.05 μM; (racemic), IC₅₀ = 0.8 +/- 0.2 μM). In contrast, (+)-**2** (aka **37**) and (+)-**5** (aka **35**) displayed no inhibition (IC₅₀ > 25 μM), indicating a fine degree of selectivity in the active site due to chiral geometry.

SAR Summary:

R₁ = substitution here does not seem well tolerated.

R₂ = NO₂, F, Br, Cl, and H all seem to have comparable activity.

R₃ = Smaller groups (e.g. Me and H) and larger groups (e.g. Ph, 4-Me-Ph) show greatly diminished activity compared to furan, thiophene and isopropyl groups.

R₄ = (in order of decreasing potency) C(O)CH₃ ~ C(O)CH₂CH₃ >>> C(O)Ph, C(O)(CH₂)₂CH₃

enantiomers: (-)-enantiomer is active, whereas (+)-enantiomer is essentially inactive (in both representative analogs).

In order to demonstrate the potential for these compounds to be utilized in more advanced biological systems (e.g. cell-based assays), we investigated various *in vitro* ADME properties of the probe compound, as shown above. This chemotype was found to have acceptable kinetic solubility, good cell permeability, and it does not appear susceptible to efflux mechanisms, such as Pgp. These predictive ADME results suggest that the molecules described above should provide utility in both cell-based assays and possibility *in vivo* models probing the effects of 12-hLO inhibition. Importantly, this particular chemotype was found to be stable over extended time periods in both assay buffer and mouse plasma. Other groups have postulated that 7-substituted-8-HQ derivatives, which contain substituted anilines in place of the amide moiety (at C-9), undergo a retro-Mannich reaction to afford a reactive species that can form a variety of covalent adducts (see Figure 3a)^{xxi}. In agreement with these findings, we too found that such analogs (aniline as opposed to amide group at C-9) were relatively unstable in both assay buffer and mouse plasma. These findings suggest that the retro-Mannich pathway appears much less facile for the amide-containing series, potentially as a result of amide nitrogen being less basic than the

corresponding aniline nitrogen. A comparable 8-HQ chemical series was reported by Wyeth researchers as ADAMTS inhibitors, which like our chemotype, contain the amide moiety at C-9. They found that the compound displayed good ADME properties (CYP inhibition and microsomal stability), supporting the notion that this subtle structural difference may have a drastic effect on the overall stability of this class of compounds^{xxii}.

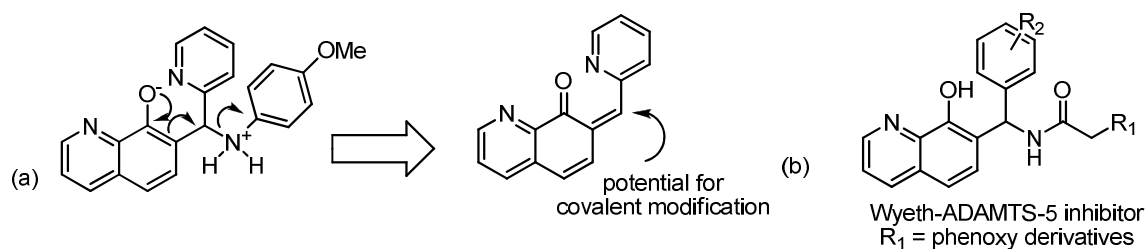


Figure 3. (a) Proposed mechanism of covalent modification for 8-HQs with aniline nitrogen at C-9

(b) Representative 8-HQ-based ADAMTS-5 inhibitor reported by Wyeth researchers with amide nitrogen at C-9.

4.1 Comparison to existing art and how the new probe is an improvement

To date, no selective small molecules for 12-hLO have been reported. Additionally, the existing art tends to be polyphenolic and generally promiscuous compounds (see above for chemical structures of existing art). In contrast, our probe compound and related analogs exhibit unprecedented selectivity against not only isozymes (5-LO, 15-LO-1 and 15-LO-2), but also related COX-1 and COX-2.

This report also details the first in-depth SAR study for inhibitors of 12-LO and the chiral separation of enantiomers that display differential activity. Our probe compound was found to be cell permeable (in Caco-2 permeability studies) and not susceptible to efflux mechanisms.

4.2 Mechanism of Action Studies

As 8-hydroxyquinoline are known metal chelators, the above data suggest that these inhibitors bind directly to the active site iron, which raises the possibility that these inhibitors could have the necessary redox potential to reduce the active ferric iron to the resting ferrous state, as has

been reported previously. To investigate the redox potential of this chemotype, DPPH, a free radical scavenger, was incubated with the probe compound; no reduction of DPPH was observed. It should be noted that stoichiometric reduction of DPPH was achieved by the known reductive LO inhibitor, NDGA, suggesting that these 8-HQ inhibitors are not reductive in nature.

Aggregation studies: Another mechanism of inhibition seen for LO is promiscuous inhibition due to small molecule aggregates. The probe compound was therefore screened with increasing amounts of Triton X-100, from 0.005% to 0.02%, with negligible changes in the IC_{50} , indicating that these compounds do not appear to aggregate.

Mode of binding: In addition to characterizing the inhibition constants, the mode of binding was investigated with steady state kinetics using the probe compound by monitoring the formation of 12-HPETE as a function of substrate and inhibitor concentration in the presence of 0.01% Triton X-100. Replots of K_M/k_{cat} and $1/k_{cat}$ versus inhibitor concentration (See Figure 4) yielded linear plots, with K_{ic} equaling $0.8 \pm 0.1 \mu M$, which is defined as the equilibrium dissociation constant. The similar affinity of inhibitor binding to both the enzyme and the enzyme substrate complex (K_{ic} is approximately K_{iu}) is a rare example of true non-competitive inhibition, which is indicative of a distal site from the catalytic site, whose inhibitor affinity is not affected by substrate binding. It should be noted that attempts to determine the reversibility of inhibition were made, but the enzyme dies too fast to allow for attempted wash-out experiments. No time-dependent inhibition was displayed when the probe compound (NCGC00183685-01/CID44460175/ML127) was incubated with 12-hLO, unlike the time-dependent inhibition seen for the bidentate catechol inhibitors against sLO-1.

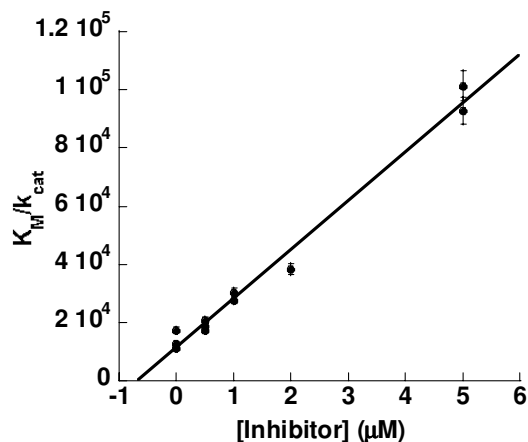


Figure 4. Steady-state kinetics data for the determination of K_{ic} for 12-hLO with inhibitor. K_M/V_{max} (slope, K_M units are μM) versus [Inhibitor] (μM) is the secondary replot of the inhibition data, which yielded a K_{ic} of $0.8 \pm 0.1 \mu\text{M}$.

4.3 Planned Future Studies

In future studies, we will aim to determine the general cytotoxicity of these compounds to obtain a TC_{50} against a variety of cell lines. Additionally, we will aim to analyze the PK properties of the molecule (mouse species) and possibly determine the maximum tolerated dose (MTD), as the reviewers expressed concerns about the toxicity of this scaffold. It should be noted that while 8-hydroquinolines are known metal chelators, which could be cause for concern, there are several marketed drugs that contain this general scaffold, for both veterinary and human use.

Since this work began, we have been contacted by several researchers in the field who have long been waiting for selective 12-LO inhibitors for their studies. Preliminary studies in their laboratory indicate that these compounds are working in cell-based systems. These efforts will be reported in due course. The experiments described above will allow us to be better informed about possibility of using these molecules as *in vivo* probes.

5 References

ⁱ Solomon, E. I., Zhou, J., Neese, F., Pavel, E. G. New insights from spectroscopy into the structure/function relationships of lipoxygenases. *Chem. Biol.* **1997**, *4*, 795-808.

ⁱⁱ (a) Brock, T. G. Regulating Leukotriene Synthesis: The Role of Nuclear 5-Lipoxygenase. *J. Cell. Biochem.* **2005**, *96*, 1203-1211. (b) Newcomer, M. E., Gilbert, N. C. Location, Location, Location: Compartmentalization of Early Events in Leukotriene Biosynthesis. *J. Biol. Chem.* **2010**, *285*, 25109-14.

ⁱⁱⁱ (a) Ghosh, J. Inhibition of Arachidonate 5-Lipoxygenase Triggers Prostate Cancer Cell Death through Rapid Activation of C-Jun N-Terminal Kinase. *Biochem. Biophys. Res. Commun.* **2003**, *307*, 342-9. (b) Ghosh, J., Myers, C. E. Inhibition of Arachidonate 5-Lipoxygenase Triggers Massive Apoptosis in Human Prostate Cancer Cells. *Proc. Natl. Acad. Sci. U. S. A.* **1998**, *95*, 13182-7. (c) Nakano, H., Inoue, T., Kawasaki, N., Miyataka, H., Matsumoto, H., Taguchi, T., Inagaki, N., Nagai, H., Satoh, T. Synthesis and Biological Activities of Novel Antiallergic Agents with 5-Lipoxygenase Inhibiting Action. *Bioorg. Med. Chem.* **2000**, *8*, 373-80.

^{iv} Radmark, O., Samuelsson, B. 5-Lipoxygenase: Regulation and Possible Involvement in Atherosclerosis. *Prostaglandins Other Lipid Mediat.* **2007**, *83*, 162-174.

^v (a) Jones, R., Adel-Alvarez, L. A., Alvarez, O. R., Broaddus, R., Das, S. Arachidonic Acid and Colorectal Carcinogenesis. *Mol. Cell. Biochem.* **2003**, *253*, 141-149. (b) Kelavkar, U. P., Cohen, C., Kamitani, H., Eling, T. E., Badr, K. F. Concordant Induction of 15-Lipoxygenase-1 and Mutant P53 Expression in Human Prostate Adenocarcinoma: Correlation with Gleason Staging. *Carcinogenesis* **2000**, *21*, 1777-1787. (c) Shureiqi, I., Lippman, S. M. Lipoxygenase Modulation to Reverse Carcinogenesis. *Cancer Res.* **2001**, *61*, 6307-6312.

^{vi} (a) Hsi, L. C., Wilson, L. C., Eling, T. E. Opposing Effects of 15-Lipoxygenase-1 and -2 Metabolites on Mapk Signaling in Prostate Alteration in Peroxisome Proliferator-Activated Receptor Gamma. *J. Biol. Chem.* **2002**, *277*, 40549-40556 (b) Shappell, S. B., Manning, S., Boeglin, W. E., Guan, Y. F., Roberts, R. L., Davis, L., Olson, S. J., Jack, G. S., Coffey, C. S., Wheeler, T. M., Breyer, M. D., Brash, A. R. Alterations in Lipoxygenase and Cyclooxygenase-2 Catalytic Activity and Mrna Expression in Prostate Carcinoma. *Neoplasia* **2001**, *3*, 287-303. (c) Shappell, S. B., Olson, S. J., Hannah, S. E., Manning, S., Roberts, R. L., Masumori, N., Jisaka, M., Boeglin, W. E., Vader, V., Dave, D. S., Shook, M. F., Thomas, T. Z., Funk, C. D., Brash, A. R., Matusik, R. J. Elevated Expression of 12/15-Lipoxygenase and Cyclooxygenase-2 in a Transgenic Mouse Model of Prostate Carcinoma. *Cancer Res.* **2003**, *63*, 2256-2267.

-
- ^{vii} (a) Brash, A. R., Boeglin, W. E., Chang, M. S. Discovery of a Second 15-Lipoxygenase in Humans. *Proc. Natl. Acad. Sci. U. S. A.* **1997**, *94*, 6148-6152. (b) Gonzalez, A. L., Roberts, R. L., Massion, P. P., Olson, S. J., Shyr, Y.; Shappell, S. B. 15-Lipoxygenase-2 Expression in Benign and Neoplastic Lung: An Immunohistochemical Study and Correlation with Tumor Grade and Proliferation. *Hum Pathol* **2004**, *35*, 840-849.
- ^{viii} (a) Suraneni, M. V., Schneider-Broussard, R., Moore, J. R., Davis, T. C., Maldonado, C. J., Li, H., Newman, R. A., Kusewitt, D., Hu, J., Yang, P., Tang, D. G. Transgenic Expression of 15-Lipoxygenase 2 (15-Lox2) in Mouse Prostate Leads to Hyperplasia and Cell Senescence. *Oncogene* **2010**, *29*, 4261-4275. (b) Tang, D. G., Bhatia, B., Tang, S., Schneider-Broussard, R. 15-Lipoxygenase 2 (15-Lox2) Is a Functional Tumor Suppressor That Regulates Human Prostate Epithelial Cell Differentiation, Senescence, and Growth (Size). *Prostaglandins Other Lipid Mediat.* **2007**, *82*, 135-146.
- ^{ix} Jobard, F., Lefevre, C., Karaduman, A., Blanchet-Bardon, C., Emre, S., Weissenbach, J., Ozguc, M., Lathrop, M., Prud'homme, J. F., Fischer, J. Lipoxygenase-3 (Aloxe3) and 12(R)-Lipoxygenase (Alox12b) Are Mutated in Non-Bullous Congenital Ichthyosiform Erythroderma (Ncie) Linked to Chromosome 17p13.1. *Hum. Mol. Genet.* **2002**, *11*, 107-113.
- ^x Hussain, H., Shornick, L. P., Shannon, V. R., Wilson, J. D., Funk, C. D., Pentland, A. P., Holtzman, M. J. Epidermis Contains Platelet-Type 12-Lipoxygenase That Is Overexpressed in Germinal Layer Keratinocytes in Psoriasis. *Am. J. Physiol.* **1994**, *266*, C243-53.
- ^{xi} Ding, X. Z., Iversen, P., Cluck, M. W., Knezetic, J. A., Adrian, T. E. Lipoxygenase Inhibitors Abolish Proliferation of Human Pancreatic Cancer Cells. *Biochem. Biophys. Res. Commun.* **1999**, *261*, 218-223.
- ^{xii} (a) Connolly, J. M., Rose, D. P. Enhanced Angiogenesis and Growth of 12-Lipoxygenase Gene-Transfected Mcf-7 Human Breast Cancer Cells in Athymic Nude Mice. *Cancer Lett.* **1998**, *132*, 107-112. (b) Natarajan, R., Nadler, J. Role of Lipoxygenases in Breast Cancer. *Front. Biosci.* **1998**, *3*, E81-88.
- ^{xiii} (a) Bleich, D., Chen, S., Gu, J. L., Nadler, J. L. The role of 12-lipoxygenase in pancreatic-cells. *Int. J. Mol. Med.* **1998**, *1*, 265-272. (b) Ma, K., Nunemaker, C. S., Wu, R., Chakrabarti, S. K., Taylor-Fishwick, D. A., Nadler, J. L. 12-lipoxygenase products reduce insulin secretion and β -cell viability in human islets. *J. Clin. Endocrinol. Metab.* **2010**, *95*, 887-893.
- ^{xiv} Catalano, A., Procopio, A. New aspects on the role of lipoxygenases in cancer progression. *Histol. Histopathol.* **2005**, *20*, 969-975.
- ^{xv} Krishnamoorthy, S., Jin, R., Cai, Y., Maddipati, K. R., Nie, D., Pages, G., Tucker, S. C., Honn, K. V. 12-Lipoxygenase and the regulation of hypoxia-inducible factor in prostate cancer cells. *Exp. Cell Res.* **2010**, *316*, 1706-1715.

^{xvi} Steele, V. E., Holmes, C. A., Hawk, E. T., Kopelovich, L., Lubet, R. A., Crowell, J. A., Sigman, C. C., Kelloff, G. J. Lipoxygenase inhibitors as potential cancer chemopreventives. *Cancer Epidemiol. Biomarkers Prev.* **1999**, *8*, 467-483.

^{xvii} (a) Jiang, W. G., Douglas-Jones, A., Mansel, R. E. Levels of expression of lipoxygenases and cyclooxygenase-2 in human breast cancer. *Prostaglandins Leukot. Essent. Fatty Acids* **2003**, *69*, 275-281. (b) Mohammad, A. M., Abdel, H. A., Abdel, W., Ahmed, A. M., Wael, T., Eiman, G. Expression of cyclooxygenase-2 and 12-lipoxygenase in human breast cancer and their relationship with HER-2/neu and hormonal receptors: impact on prognosis and therapy. *Indian J. Cancer* **2006**, *43*, 163-168. (c) Zeeneldin, A. A., Mohamed, A. M., Abdel, H. A., Taha, F. M., Goda, I. A., Abodeef, W. T. Survival effects of cyclooxygenase-2 and 12-lipoxygenase in Egyptian women with operable breast cancer. *Indian J. Cancer* **2009**, *46*, 54-60.

^{xviii} Michael, S.; Auld, D.; Klumpp, C.; Jadhav, A.; Zheng, W.; Thorne, N.; Austin, C. P.; Inglese, J.; Simeonov, A. A robotic platform for quantitative high-throughput screening. *Assay Drug Dev Technol* **2008**, *6*, 637-657.

^{xix} Pierre, J. L., Baret, P., Serratrice, G. Hydroxyquinolines as Iron Chelators. *Curr. Med. Chem.* **2003**, *10*, 1077-1084.

^{xx} (a) Liu, Z. D., Kayyali, R., Hider, R. C., Porter, J. B., Theobald, A. E. Design, Synthesis, and Evaluation of Novel 2-Substituted 3-Hydroxypyridin-4-Ones: Structure-Activity Investigation of Metalloenzyme Inhibition by Iron Chelators. *J. Med. Chem.* **2002**, *45*, 631-639. (b) Nelson, M. J., Brennan, B. A., Chase, D. B., Cowling, R. A., Grove, G. N., Scarrow, R. C. Structure and Kinetics of Formation of Catechol Complexes of Ferric Soybean Lipoxygenase-1. *Biochemistry* **1995**, *34*, 15219-15229.

^{xxi} McLean, L. R., Zhang, Y., Li, H., Li, Z., Lukasczyk, U., Choi, Y. M., Han, Z., Prisco, J., Fordham, J., Tsay, J. T., Reiling, S., Vaz, R. J., Li, Y. Discovery of Covalent Inhibitors for Mif Tautomerase Via Cocrystal Structures with Phantom Hits from Virtual Screening. *Bioorg. Med. Chem. Lett.* **2009**, *19*, 6717-6720.

^{xxii} Gilbert, A. M., Bursavich, M. G., Lombardi, S., Georgiadis, K. E., Reifenberg, E., Flannery, C. R., Morris, E. A. N-((8-Hydroxy-5-Substituted-Quinolin-7-Yl)(Phenyl)methyl)-2-Phenoxy/Amin O-Acetamide Inhibitors of Adamts-5 (Aggrecanase-2). *Bioorg. Med. Chem. Lett.* **2008**, *18*, 6454-7.